

# Role of Alpha Oscillations During Short Time Memory Task Investigated by Graph Based Partitioning

Cagatay AYDIN<sup>1</sup>, Oytun OKTAY<sup>3</sup>, Adem Umut GUNEBAKAN<sup>1</sup>,  
Ahmet ADEMOGLU<sup>1</sup>, Rifat Koray CIFTCI<sup>2</sup>

<sup>1</sup>Institute of Biomedical Engineering, Bogazici University, Kandilli Campus, Cengelkoy/ Istanbul, 34684 Turkey

<sup>2</sup>Department of Biomedical Engineering, Namik Kemal University, Corlu/ Tekirdag, 59860 Turkey

<sup>3</sup>Dept. of Electronics and Telecommunication Engineering, Namik Kemal University, Corlu/ Tekirdag, 59860 Turkey

cagatay.aydin@boun.edu.tr, moktay@nku.edu.tr, adem.gunebakan@boun.edu.tr,  
ademoglu@boun.edu.tr, kciftci@nku.edu.tr

**Abstract.** *In this study, we investigate the clustering pattern of alpha band (8 Hz - 12 Hz) electroencephalogram (EEG) oscillations obtained from healthy individuals during a short time memory task with 3 different memory loads. The retention period during which subjects were asked to memorize a pattern in a square matrix is analyzed with a graph theoretical approach. The functional coupling among EEG electrodes are quantified via mutual information in the time-frequency plane. A spectral clustering algorithm followed by bootstrapping is used to parcellate memory related circuits and for identifying significant clusters in the brain. The main outcome of the study is that the size of the significant clusters formed by alpha oscillations decreases as the memory load increases. This finding corroborates the active inhibition hypothesis about alpha oscillations.*

## Keywords

EEG, brain, graph theory, memory, spectral clustering, information theory.

## 1. Introduction

A big question comes to a mind that how functional brain stages arise from the interaction of many different brain regions in a complex harmony. From the references of much evidence that are relevant for neuroscientist, complex brains can deal with information which consists of real time, highly rapid interactions between sensory channels and formerly specified brain regions [24]. The sophisticated architecture of brain networks can be observed with the help of spectral clustering analysis to parcellate functional interaction between regions like clusters and the directions of information flow from one cluster to another. An EEG device has robust temporal resolution which is an outstanding property to observe visual stimulus and event related signal variability due to highly rapid fluctuation characteristic.

Klimesch et al. [10] came with the assumption of investigating memory related brain dynamics with respect to dynamic property of memory processing. In addition, previous studies suggested that, the alpha band and its oscillatory components could be a bridge between thalamus and cortex which was affected by the synchronized neural activity [3]. From his assumption, if the memory processing is using the longitudinal pathways (feedback loops) which link the thalamic nuclei with the cortex, one of the most predominant rhythm alpha (8 – 12 Hz) can be used to extract the memory information in these pathways. Thus, alpha band oscillations and signal power varieties of the EEG rhythm are investigated with respect to the working memory (WM) composition of over all brain dynamics [8], [9], [10], [11], [12], [17], [19], [25]. To observe the memory load brain circuitry several event related desynchronization (ERD) [10] and event related potential (ERP) [6] studies are implemented. The EEG oscillatory information during memory load task is observed in several studies [8], [25], [9]. There are two competing theories for the role of alpha oscillations in the brain: One theory suggests that alpha oscillations actively inhibit the brain regions that are not involved in the actual cognitive task [8], whereas the other states that these oscillations take part in the formation of cognitive networks directly related with the performed task [17].

In previous studies, information theoretic measures are used to estimate mutual information (MI) of the time delays between EEG electrode pairs [15], mean phase coherence of phase synchronization for detecting epileptic activity [16], orthogonal wavelet transform (ODWT) in order to overcome by the non-stationary characteristic of the EEG signal [18] and entropy difference method for classification accuracy in brain computer interface (BCI) study [21]. In order to analyze both time and frequency components of an EEG signal by using information theoretic measures, time-frequency distributions (TFD) are consistent measures. The dependencies between signal pairs on time-frequency plane can be quantified with a measure like mutual information (MI). Hence, to generate the statistical difference between

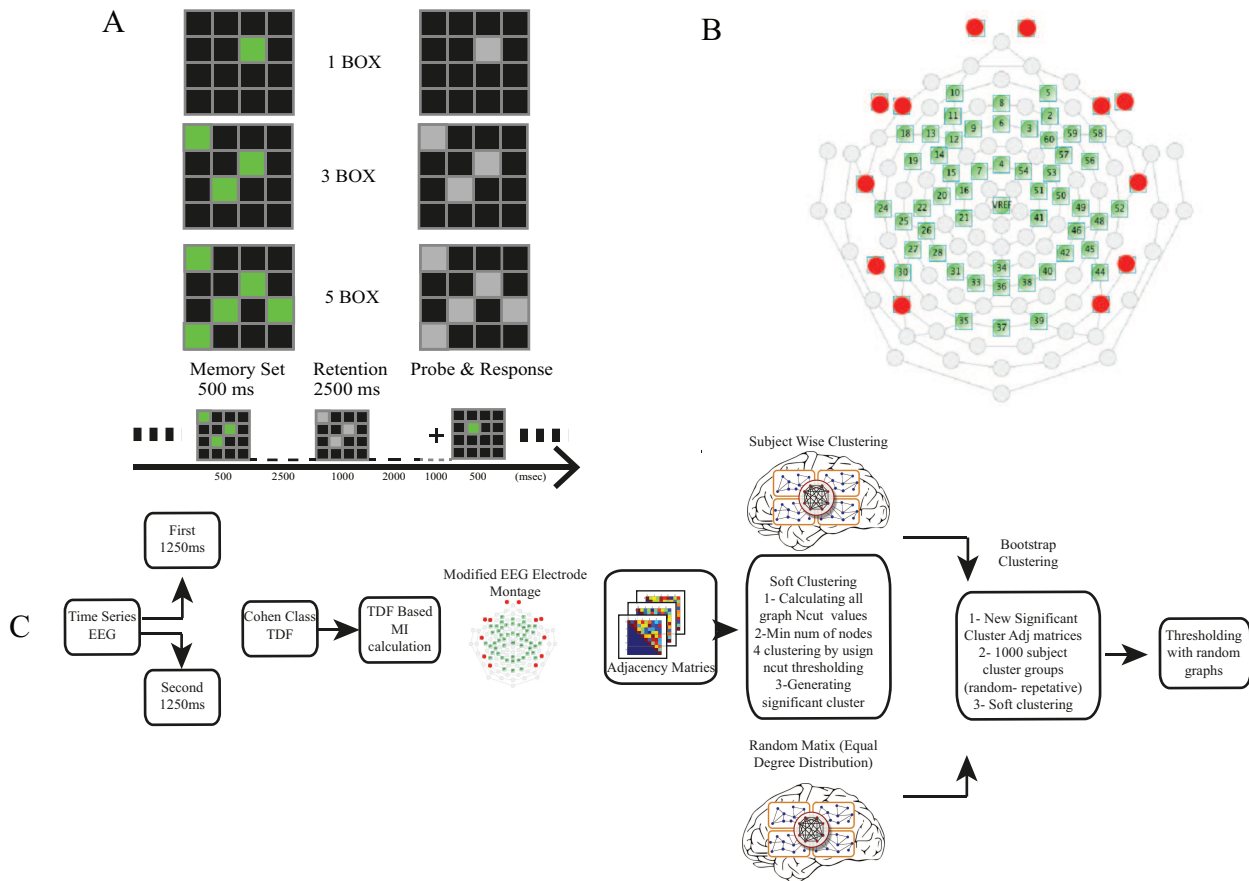


**Fig. 1.** (A) The representation of the visuospatial memory task, (B) Topological view of EEG electrode montage locations and red dots are used to initialize the electrode elimination process, (C) Flow diagram of the entire analytical process.

signal pairs, individual TFDs and a joint TFD of a signal pair is adequate enough to calculate the time-frequency based MI [1], [2]. A recent study used the time-frequency cross mutual information analysis to inquire the functional connectivity in alpha and the beta bands during resting, preparing, movement onset and movement offset states [13].

Several scientific fields have similar purposes to separate their data in groups which consist of interrelated components. Spectral clustering has manifest advantages among varieties of clustering methods due to its implementation ease, calculation efficiency and enhancement of traditional clustering algorithms such as k-means. In previous clustering studies, the eigenvalues and the eigenvectors of the un-normalized Laplacian matrix are used to distinguish the properties of graphs. Furthermore, second eigenvector of the Laplacian matrix is used to detect bi-partitions of the graph [14]. Shi et al. referred to a normalized cut algorithm as an unbiased measure which allowed to establish a sub-group of a graph by minimizing normalized cut with maximizing the similarity within the cluster [23]. The main reason why the spectral clustering technique is used in the bi-partitioning of varieties of a signal type is that, it does not make strong assumptions on the form of clusters. There are several fMRI

studies which have observed the resting state network properties [22], [27], and brain tumor separation [7], by using the n-cut algorithm.

The main contribution of this study relies on integrating a system as a pre-diagnostic tool in which one could observe the ongoing memory networks for memory-related brain disorders. The paper is organized as follows: Section 1 gives detailed information about the EEG signal characteristics due to the specified EEG band intervals. In addition, cognitive brain networks related to memory processing and short time memory load are introduced. The information theoretic measures are briefly explained and time-frequency based (Cohen Class) mutual information is explained. At the end of the Section, the graph based spectral clustering algorithm is briefly explained in EEG signal processing. The detailed approximation of methods and our experimental design are explained in Section 2. The preprocessing procedure, information theoretic measures and their calculations, the formulation of *N*-Cut clustering are presented. Moreover, the soft clustering method is introduced and presented in detail. In Section 3, behavioral and soft clustering results are presented. In Sections 4 and 5, discussions and conclusions are given, respectively.

## 2. Materials and Methods

### 2.1 Experiment Design

In this experiment, the EEG data was recorded over 17 (13 male, 5 female, mean age of 23) healthy subjects. Experimental procedure was applied as voluntarily and participants signed an informed consent about their medical history in order to exclude those subjects who might have brain related disorders.

The visuo-spatial short time memory task (Fig. 1(A)), adapted from Sauseng et al. [19] was run after the locations of one, three or five targets on four by four box model were shown to the subjects for 500 milliseconds. During each stimulus, one of three box combinations (one, three or five box) was represented randomly. Due to the box combination model, their positions had to be kept in memory for 2,500 milliseconds and had to be compared with an answer stimulus which was presented in gray color. A comparison should be made between the probe and the answer stimulus to decide on whether the target positions were exactly the same as answer positions or not. After 2,500 milliseconds retention interval, if it was true, subjects had to answer with the right mouse button press or vice versa in 1000 milliseconds. To be able to preserve the event synchronization, the clock in the data recording computer and the clock in the experiment computer were synchronized periodically after each trial.

The segmentation period for this experiment was 4000 ms. Each segment was started from 500 ms after the probe (green) stimulus to 1000 ms after the answer stimulus (gray). The significant time interval for each segment which was 2500 ms long between the probe and the response, was used in analysis. Furthermore, the main reason for initializing longer time interval in segmentation was to secure the signal from fluttering in the filtering of preprocessing analysis. Each answer, each reaction time, and the overall mean reaction time for each box model was calculated and written into a log file.

There were 100 stimuli for each box combinations and there were equal number of true and false probes. In total, 300 stimuli were represented during the experiment. Only correct answers were taken into consideration. The experimental design was made by the Psycotoolbox, Matlab software.

#### 2.1.1 Data Acquisition and EEG Preprocessing

EEG recordings were done by 64 channel EGI Hydro-Cel amplifier and the ongoing recordings were stored on Macintosh Workstation computer. To establish the impedance levels which were set as 50 k $\Omega$ , sponge electrodes were soaked in potassium chloride and alcohol free shampoo solution for about 10 min before the cap placement. The preprocessing steps can be listed as; 0.1 Hz first order high pass filtering, 100 Hz low pass filtering, 50 Hz Notch filtering, segmentation of correct segments, artifact detection, ocular artifact removal, bad channel replacement and file

export. The preprocessing was done with EGI Net Station software tools.

### 2.2 Information Theoretical Analysis on Time-Frequency Plane

To calculate both time and the frequency components of the signal, Cohen class distributions can be calculated. The main formula of Cohen's class  $C(t, f)$  can be expressed as;

$$C(t, f) = \left( \int \int \int \phi(\theta, \tau) s\left(u + \frac{\tau}{2}\right) s^*\left(u - \frac{\tau}{2}\right) e^{j(\theta u - \theta t - 2\pi f \tau)} du d\theta d\tau \right). \quad (1)$$

The  $s$  represents the signal,  $s^*$  represents complex conjugate of the given signal and  $\phi(\theta, \tau)$  stands for the kernel function. The energy preservation and marginals which are the properties of time frequency distributions (TFD) are satisfied:

The conversion of information theoretic measures such as entropy into TFDs representation can be accomplished by (3),

$$\int \int C(t, f) dt df = \int |s(t)|^2 dt = \int |S(f)|^2 df, \quad (2)$$

$$\int C(t, f) df = |s(t)|^2, \int C(t, f) dt = |S(f)|^2. \quad (3)$$

PDFs and TFDs are different from each other for that, TFDs are not always positive like as PDFs. Hence, in this study spectrograms which are always positive, are used for generating Cohen class TFDs. Moreover, before the implementation for information theoretical based measures, TFD has to be normalized by its energy distribution. Cohen class TFDs are calculated by using TFTB, Matlab software.

#### 2.2.1 Time-Frequency Plane Mutual Information

For a brief approximation of one dimensional mutual information (MI) calculation, assume that two random variables  $X$  and  $Y$  have mutual information which can be expressed as;

$$I(X; Y) = \sum_x \sum_y p(x, y) \log \frac{p(x, y)}{p(x)p(y)}. \quad (4)$$

Here,  $p(x, y)$  is a joint probability density function and  $p(x)$  and  $p(y)$  are marginal PDFs of  $X$  and  $Y$ . If  $X$  and  $Y$  are independent from each other, MI is determined as minimum and equal zero.

To calculate Cohen class TFD with the help of Cohen class distribution, energy density functions are taken into account instead of PDFs. If we replace the marginal densities  $p(x), p(y)$  with the individual energy densities  $C_x(t, f), C_y(t, f)$  and the joint PDFs  $p(x, y)$  with the joint energy distributions  $C_{xy}(t, f)$  the main equation (4) can be formed.

The MI equation (4) can be computed by;

$$I(C_x, C_y) = \int \int |C_{xy}(t, f)| \log \frac{|C_{xy}(t, f)|}{C_x(t, f) C_y(t, f)} dt df. \quad (5)$$

### 2.3 Graph Based Soft Clustering

A significant drawback of existing clustering algorithms is determining the number of clusters beforehand. Most of the time it is not possible to define an optimum and this determination is done with heuristic methods. Additionally, when the task is determining the group-wise clusters from individual subject level clusters, setting the cluster number to the same value for all subjects and the group may restrict the inference that might be obtained from this large group of data. Hence, to introduce some flexibility and circumvent the problem of setting a fixed cluster number, a soft clustering approach (Fig. 1(C)) may be adopted. The method is based on the successive application of the clustering algorithm to the clusters that are obtained at earlier steps. The rationale is that if two nodes have a strong inter-connection then they will be separated at later levels of these successive clusterings, but if they have a weak connection they will be segregated at earlier steps.

#### 2.3.1 N-cut Clustering Algorithm

A network is represented with the help of nodes or vertices and the edges between these nodes. The directed and undirected graph can be represented as follows;

The vertices and edges can be represented as  $V = \{v_1, v_2, \dots, v_n\}$ , if the edges are connected in terms of the MI results  $e(i, j) = 1$  otherwise  $e(i, j) = 0$ . The graph can be represented as  $G(V, E)$  [22].

If the graph is considered as a weighted graph, the adjacency matrix can be represented by  $W = ((w_{ij})_{i, j = 1, \dots, n})$ , then the  $w_{ij} = 0$  means that there is not a connection between  $v_i, v_j$  otherwise, it carries non-negative value  $w_{ij} \geq 0$ .

The degree of a matrix can be defined as

$$d_i = \sum_{j=1}^n w_{ij}. \quad (6)$$

In this particular notation, this sum indicates that sum of all  $v_j$  vertices are adjacent to  $v_i$ . Degree matrix  $D$  is defined as a diagonal matrix which includes the sum of edges attached to given vertices  $d_1, \dots, d_n$  [14].

The number of vertices is used to measure the size of partition  $A$ . On the other hand,  $vol(A)$  measures the size in terms of summation over the weights of all edges which are attached to vertices in  $A$ . The size of the partition can be described in two ways;

$$\begin{aligned} |A| &= \text{the number of vertices in } A, \\ vol(A) &= \sum_{i \in A} d_i. \end{aligned} \quad (7)$$

N-cut algorithm can be described as

$$Ncut(A, \bar{A}) = \frac{cut(A, \bar{A})}{vol(A)} + \frac{cut(A, \bar{A})}{vol(\bar{A})}, \quad (8)$$

$$cut(A, \bar{A}) = \sum_{v_i \in A, v_j \in \bar{A}} w(i, j). \quad (9)$$

According to Shi and Malik [23], normalized spectral clustering algorithm can be listed as follows;

- The number of clusters  $k$  clusters is selected.
- The un-normalized Laplacian is computed by:  
 $L = D - W$ .
- Due to number of  $k$  clusters,  $u_1, \dots, u_k$  eigenvectors are computed with the help of generalized formula  $Lu = \lambda Du$  and those eigenvectors corresponding to the  $k$  largest eigenvalues are selected.
- The  $U \in R^{n \times k}$  matrix is generated by using  $\mathbf{u}_1, \dots, \mathbf{u}_k$  eigenvectors as columns.
- For  $i = 1, \dots, n$ , the  $y_i \in R^k$  vector is obtained as the  $i$ -th row of  $U$  matrix.
- The  $y_i$  in  $R^k$ ,  $i = 1, \dots, n$  are clustered in with the  $k$ -means algorithm into clusters  $C_1, \dots, C_k$  [14].
- The clusters  $A_1, \dots, A_k$  with  $A_i = \{j | y_j \in C_i\}$  are generated.

#### 2.3.2 Soft Clustering Algorithm

The  $N$ -cut clustering algorithm is applied to the adjacency matrix  $W$  by choosing the symmetric version of the normalized  $L$  matrix,  $L_{sym}$ . At any particular level, existing clusters are partitioned individually and the global  $N$ -cut values for these candidate clusters are computed. Then, the cluster which gives the minimum  $N$ -cut value is partitioned. This procedure continues until all the clusters have at most 6 nodes. At each partitioning step a cluster identity vector is formed and written in a matrix form. After the termination of the procedure, these cluster identity matrices are averaged and a resultant matrix which represents clustering strength between any two nodes is obtained. This matrix has values between 0 and 1, and a value near 1 signifies that those two nodes are highly likely to be clustered together, whereas a value near 0 notifies that those two nodes can hardly be clustered within the same cluster. As a result, this procedure gives us a new interaction matrix generated from the adjacency matrix, but this time the interaction strength between two nodes is computed from the probability of being clustered together.

In Fig. 2(A), tree shaped decomposition represents the  $N$ -Cut value computation for the all possible end clusters in a given graph. In other words, a road map with respect to clustering information of the whole graph is computed. In this study, subject-wise and group-wise adjacency matrices have low-sized matrix formation such as  $52 \times 52$  which allows us to implement  $N$ -Cut analysis with computational ease.

- Using  $N$ -cut values  $l_1, \dots, l_l$  of  $N$ -Cut index  $N_N$  is used as a computation threshold for the generalized  $N$ -cut algorithm.

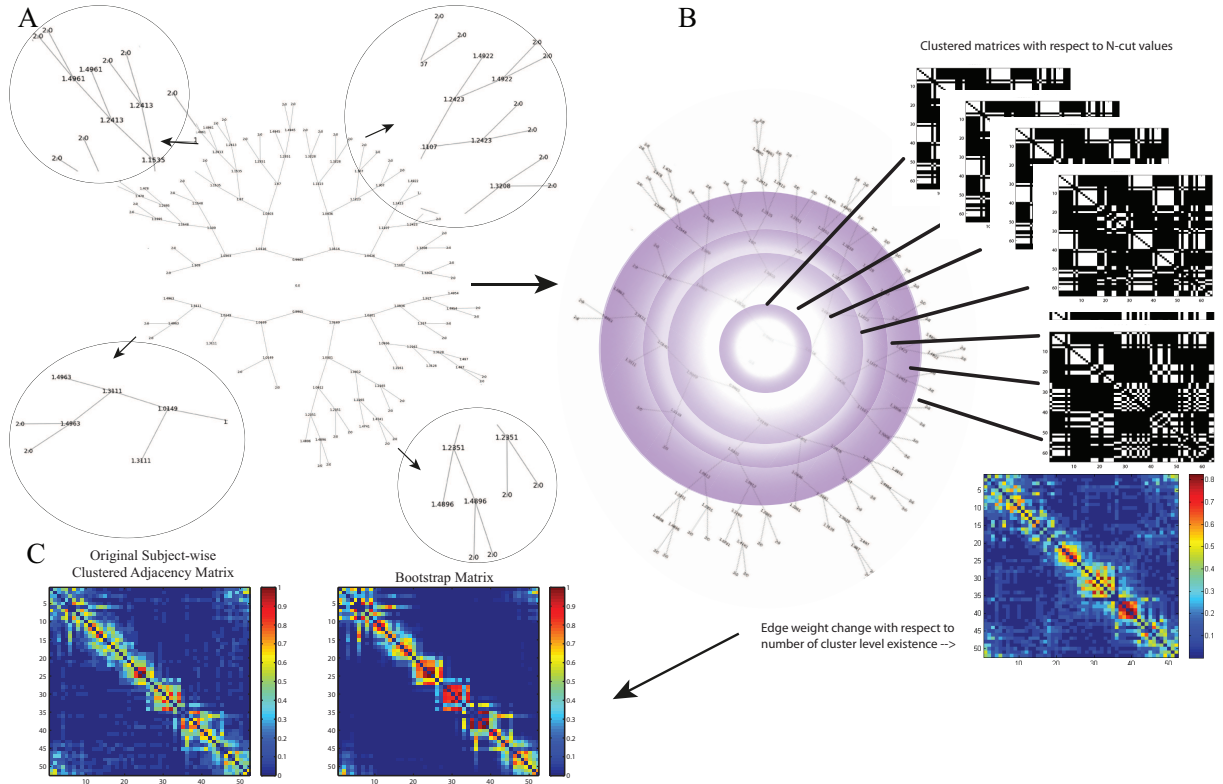


**Fig. 2.** (A) Soft Clustering N-cut value decomposition of a graph, (B) Soft Clustering: Generation of adjacency matrices with respect to node-cluster existence, (C) (Left) Original Group-wise Adjacency Matrix (Right) Bootstrap Adjacency Matrix.

- The cluster vectors  $A_1, \dots, A_k$  of a specific  $N$ -cut value are merged by multiplying each  $A_i$  with its cluster index  $i$  to form the vector  $N_S = [1.A_1 + \dots + k.A_k]$ .
- The  $N$ -cut value based clustered matrix  $S_S \in R^{s \times n}$  for number of  $N$ -cut values is generated as  $S_S = [(N_S)_1, \dots, (N_S)_s]$ .
- The 3-D prone matrix  $P_S \in R^{n \times n \times L}$  is generated by taking each column of  $S_S$  and mapping its indices as (10)

$$P_S(i, j, s) = \begin{cases} 1 & \text{if } S_S(s, i) = S_S(s, j), \\ 0 & \text{else.} \end{cases} \quad s = 1, \dots, 17, \quad (10)$$

- The mean of 2-D prone matrix  $P_S \in R^{n \times n}$  is generated to form the 2-D subject prone matrix.

The algorithm is calculated for all subjects ( $s = 17$ ), two time intervals (0 ms - 1250 ms, 1250 ms -2500 ms) and 3 task conditions (1, 3 and 5 box combination).

This group-wise analysis is repeated over three task conditions i.e. 1, 3 and 5 box combination and clustering information is topologically plotted over modified electrode locations to investigate the comparison between different box models.

### 2.3.3 Bootstrap Statistical Test

In order to identify statistically significant electrodes from group-wise clusters, bootstrap technique is employed

[4]. The 2D slabs of the  $P_S$  matrix are shuffled with the repetition allowed manner to obtain its surrogate versions. 1000 trials of  $P_S$  are obtained from a sequence of indices uniformly distributed between (1 – 17) which give the shuffled indices of the slabs. The indices allow for a slab to appear more than once.

The shuffled  $P_S$  is fed into generalized Soft clustering algorithm 1000 times and the average cluster matrix is thresholded by 95 % of its maximum value and the entries exceeding it are plotted on the scalp as statistically significant nodes.

## 3. Results

### 3.1 Behavioral Results

During the experiment, the visuo-spatial stimulus information, subject response information and reaction times were recorded into a log file. In addition, the percentage of correct answers, the mean reaction time, fastest reaction time were calculated and added into log file. To compare the reaction time and error percentage between 3 different task conditions, mean reaction times and mean error rates of all subjects were computed (Fig. 3).

There was no statistically significant difference in correct responses between 3 box and 5 box model ( $\%92.9 \pm 4.6$ ) ( $p = 0.811$ ). However, there were significant differences between 1 box ( $\%94.8 \pm 4.0$ ) and 3 box model

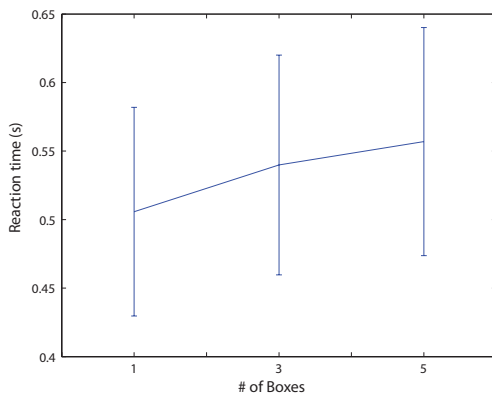


Fig. 3. 3 Box model mean reaction time comparison.

( $93.13 \pm 5.3$ ) ( $p = 0.050$ ) and between 1 box and 5 box model ( $p = 0.0030$ ).

Directly proportional reaction time increase was observed by the number of represented boxes. The mean reaction time due to box models can be listed as follows; 1 box model  $0.50 \pm 0.07$ , 3 box model  $0.53 \pm 0.08$ , 5 box model  $0.55 \pm 0.08$  seconds. There were significant differences between 1 box and 3 box model ( $p = 0.00047$ ), between 1 box and 5 box model ( $p = 0.000046$ ), 2 box and 3 box model ( $p = 0.0067$ ).

### 3.2 Experimental Results

In the soft clustering approach, only modified electrode montage (Fig. 1(B)) is used to determine mutual information based adjacency matrices. With respect to modified electrode locations, Soft Clustering algorithm is implemented over subjects with respect to the change in two time intervals and three task conditions. Using (8), Laplacian vectors are computed to determine normalized cut values of the graph. Hence, the  $N$ -Cut values which are used to cluster the graph into sub-graphs are computed for all clustering levels using (9). For each subject adjacency matrix is repetitively clustered for all previously calculated  $N$ -Cut values which can be considered as using  $N$ -Cut value to threshold the level of cluster computation. In addition, clustered adjacency matrices are saved to determine subject-wise soft clustering matrix. Subject-wise soft clustering matrix is calculated from the number of node existence within a specific cluster. Thus, if a node is eager to exists in the same cluster at various clustering levels, edge weights are supposed to be high valued. The mentioned procedure is repeated over each experiment condition and two time intervals.

Over 17 subject-wise soft cluster matrices, 1000 pseudo subject-wise soft cluster matrix combinations are generated. Pseudo combinations which can comprise repetitive sequences are randomly distributed. After the generation of simulation database, overall mean is calculated over subject-wise soft clusters ( $1000 \times 17 \times 52 \times 52$ ), and for further soft clustering analysis, 1000 group clusters ( $1000 \times 52 \times 52$ ) are generated. Similarly, to implement group-wise

soft clustering analysis, from each subject-wise soft clustered matrix in simulation database,  $N$ -Cut values are computed. Minimum number of nodes inside the end clusters are set to four and group-wise soft clusters are generated with the help of previously computed  $N$ -Cut thresholds.

After the procedure of subject-wise and group-wise soft clustering approach, clustering information is plotted over maps with respect to two different time intervals and three different task conditions. In addition, after group-wise soft clustering, all connections between various clusters can be observed. In Fig. 4, maps *A*, *C* and *E* are representing first 1250 ms time interval in the retention period for 1, 3 and 5 box combinations, respectively. The statistically significant nodes which are computed from the bootstrapped group-wise clusters are projected over the maps and indicated as red color. Both original and statistically significant node sizes on the maps are changing due to the degree values (number of intra-cluster edges connected to a given node) which are obtained by using (6). First of all, with respect to the memory load, the number of soft clusters are decreasing (for *A* and *C*; 6 different clusters, for *E*; 5 different clusters) proportional to the number of boxes which are represented in the probe stimulus. In the first time interval, the organization of prefrontal clusters are observed as the same formation for varying memory load. However, the degree values of the the nodes and the number of statistical significant nodes located over prefrontal region are decreasing over the increasing memory demand (see clusters 1, 4 and 3 in Fig. 4 *A*, *C* and *E*). On the other hand, in maps *A* and *C*, the formation of right-lateral parietal region can be observed as two separate clusters and in map *E*, they formed a larger cluster by the memory load (see cluster 5). The increase in the degree of the nodes inside the clusters can be observed over occipital region in map *E*.

In *B*, *D*, *F* maps, the second 1250 ms time interval in the retention period for 1, 3 and 5 box combinations can be observed. The clusters over the prefrontal region show similar formations. Different type of cluster organizations over the bilateral and occipital region can be observed by the varying memory load. For instance, the map *D*, 3 different clusters over the bilateral and occipital regions. However, in map *E*, the combination of clusters projected over left-lateral and occipital region (see cluster 2) can be observed. Contrarily, in map *F*, larger cluster can be observed as a combination of right-lateral and occipital region (see cluster 5). Furthermore, there are several statistically significant electrodes over left and right lateral region in map *D*. On the other hand, high degree statistically significant electrodes can be observed over occipital and left lateral region in map *F*.

## 4. Discussion

In Fig. 4, shows the difference between 1, 3, 5 box models via mean reaction time values. Ole Jensen [8] assumed that difference in the mean reaction time can be con-

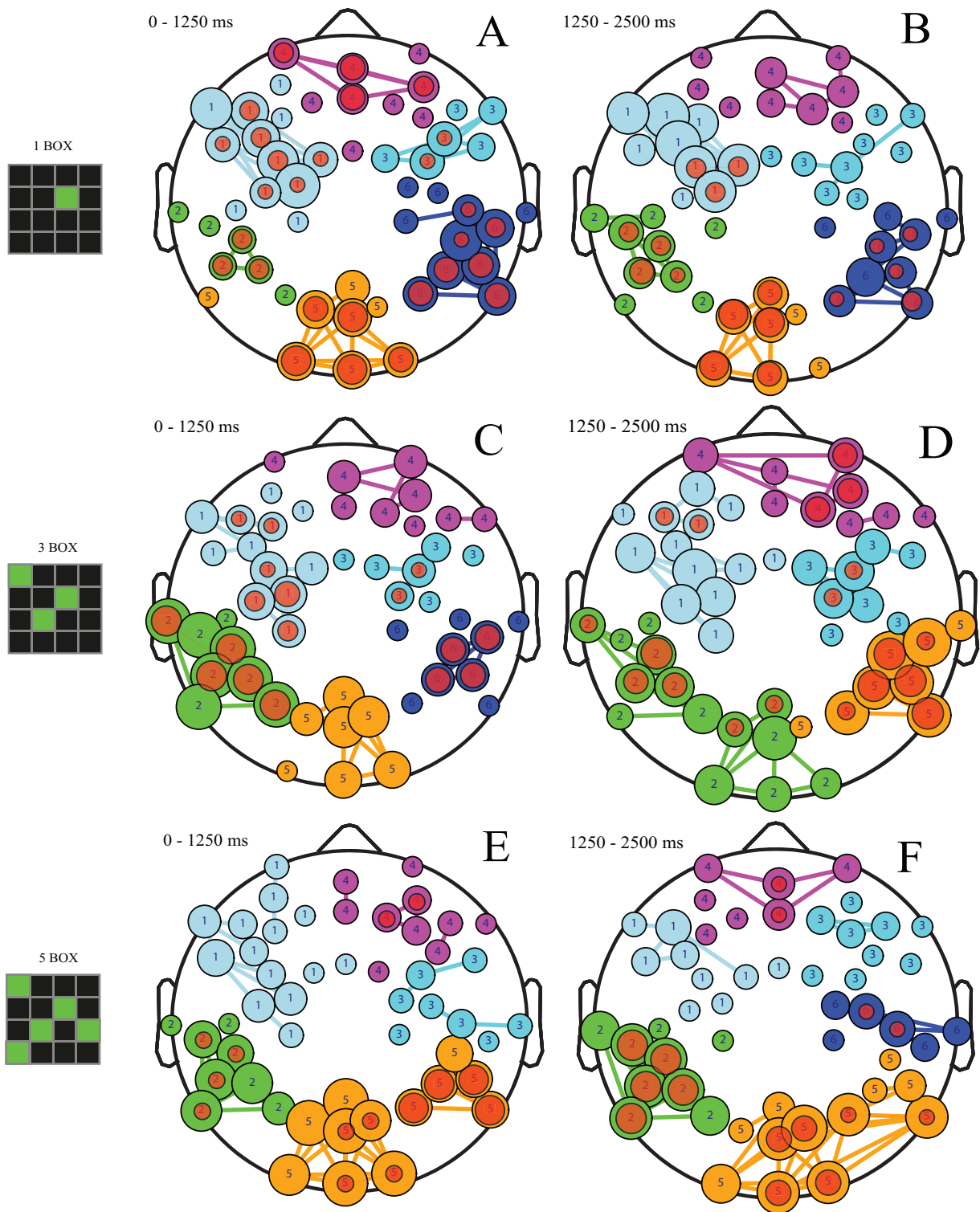


**Fig. 4.** Soft Clusters with respect to random graph threshold, *A – C – E* representing first time interval in 3 different memory load tasks (retention 1 box, retention 3 box, retention 5 box), *B – D – F* representing second time interval in 3 tasks (node sizes are changing due to the degree variations which is obtained by using (6)). The statistically significant nodes which are computed from the bootstrapped group-wise clusters are projected over the maps and indicated as red color. Both original and statistically significant node sizes on the maps are changing due to the degree values (number of intra-cluster edges connected to a given node) which are obtained by using (6).

sidered as a function of memory load. Our experiment design revealed an increase of mean reaction time due to the increase in the number of boxes.

In this study, we investigated the clustering information of memory related brain networks. There are several alpha band related studies with respect to the memory load and its reflection on the alpha band. Tuladhar et al. investigated that, a parametric increase in the alpha band activity over posterior brain areas were observed with the memory load [26]. As shown in Fig. 4, maps *C*, *E* and *F*, modified electrode locations and their statistically significant nodes provide support for the previous studies. In other words, with increasing memory demand, the size of clustered nodes which are projected on the occipital and bilateral regions increases. For instance, in map *C*, a cluster which is projected over right lateral and occipital regions can be observed. Jensen and his colleagues [8] assumed that there could be separate memory related sources which were located on the posterior and bilateral regions of the brain. They have stated that memory load could produce enhancements in the posterior and lateral regions of the brain. In addition, they inferred that the memory load activity in the separate brain regions could reflect the degree of synchronization across multiple brain regions involved. In map *E*, the nodes over the left lateral and occipital region form a huge cluster and in map *E*, the similar organization can be observed as a combined cluster of right lateral and occipital regions. Furthermore, in map *F*, degree of statistically significant electrodes over occipital region and left lateral region and in map *D*, can be observed as high valued. These combined cluster formations may indicate the spatial organization of increasing memory demand.

The parametric power increase in the first time interval with respect to the memory load was reported in the posterior regions of the brain. This can be linked to the active inhibition of neural activity [9], [12]. There are several PET and fMRI experiments that have previously indicated that several prefrontal and parietal regions are involved in the working memory maintenance. In Fig. 4 during the first time interval, number of statistically significant nodes in the prefrontal region is decreasing with respect to the memory load (see cluster 1, 4 and 3) which can be described as an inhibition of neural anterior activity [20]. In Fig. 4 from *B* to the *F* maps, there are statistically significant nodes over the left lateral regions and the degree values (intra-cluster connections) are increased by the increased memory demand which may provide evidence for the previously mentioned study [19].

## 5. Conclusion

The brain has a complex structure and a complex functioning capability. Band and region specific studies are made to observe the overall brain function. Generally, oscillations of alpha (8 Hz - 12 Hz) band of the EEG rhythm and the amplitude of the signal changes in the memory and cognitive

based tasks are observed. Furthermore, to obtain local and global interaction of memory processing, clustering analysis can be considered as important studies.

The sophisticated architecture of brain networks can be observed with the help of spectral clustering algorithm to create the dynamic interactions between regions like clusters and the directions of information flow from one cluster to another. In this study, a spectral clustering algorithm was used to parcellate memory related circuits in the brain in a load-dependent manner. To be able to circumvent the problem of choosing the number of clusters beforehand a soft clustering approach was implemented. To investigate both the spatial and the temporal change in terms of functional dynamics on the brain, EEG-fMRI fusion studies are incorporated into our ongoing schedule. Since the fMRI part of the future project consists of huge raw databases to cluster, our proposed method, the soft clustering algorithm, has to be updated with respect to computational ease and time.

In the end, the main future work will rely on developing an enhanced soft clustering algorithm which will be used as an intermediary tool to establish the link between the temporal and the spatial functional dynamics of the brain.

## Acknowledgements

This study is supported by Scientific and Technological Research Council of Turkey (TÜBİTAK) under project number 109E202.

## References

- [1] AVIYENTE, S. A measure of mutual information on the time-frequency plane. In *IEEE International Conference on Acoustics, Speech, and Signal Processing (ICASSP)*. Philadelphia (PA, USA), 2005, vol. 4, p. iv - 481.
- [2] AVIYENTE, S. Information-theoretic signal processing on the time-frequency plane and applications. In *Proceedings of 2005 European Signal Processing Conference (EUSIPCO)*. Antalya (Turkey), 2005, p. 4 - 8.
- [3] BASAR, E., DEMIRALP, T., SCHURMANN, M., BASAR-EROGLU, C., ADEMOGLU, A. Oscillatory brain dynamics, wavelet analysis, and cognition. *Brain and Language*, 1999, vol. 66, no. 1, p. 146 - 183.
- [4] BELLEC, P., MARRELEC, G., BENALI, H. A bootstrap test to investigate changes in brain connectivity for functional MRI. *Statistica Sinica*, 2008, vol. 18, 1253 - 1268.
- [5] BELLEC, P., ROSA-NETO, P., LYTTTELTON, O. C., BENALI, H., AND ALAN, C. Supplementary materials for Multi-Level Bootstrap Analysis of Stable Clusters in Resting-State fMRI. *Journal of Non-parametric Statistics*, 2010.
- [6] BUSCH, N. A., HERRMANN, C. S. Object-load and feature-load modulate EEG in a short-term memory task. *NeuroReport*, 2003, vol. 14, no. 13, p. 1721 - 1724.
- [7] CHEN, V., RUAN, S. Graph cut based segmentation of brain tumor from MRI images. *International Journal on Sciences and Techniques*

- of *Automatic Control & Computer Engineering*, 2009, vol. 3, no. 2, p. 1054 - 1063.
- [8] JENSEN, O., GELFAND, J., KOUNIOS, J., LISMAN, J. E. Oscillations in the alpha band (9-12 Hz) increase with memory load during retention in a short-term memory task. *Cerebral cortex*, 2002, vol. 12, no. 8, p. 877 - 882.
- [9] JOKISCH, D., JENSEN, O. Modulation of gamma and alpha activity during a working memory task engaging the dorsal or ventral stream. *The Journal of Neuroscience: The Official Journal of the Society for Neuroscience*, 2007, vol. 27, no. 12, p. 3244 - 3251.
- [10] KLIMESCH, W. EEG-alpha rhythms and memory processes. *International Journal of Psychophysiology: Official Journal of the International Organization of Psychophysiology*, 1997, vol. 26, no. 1-3, p. 319 - 340.
- [11] KLIMESCH, W. EEG alpha and theta oscillations reflect cognitive and memory performance: A review and analysis. *Brain Research: Brain Research Reviews*, 1999, vol. 29, no. 2-3, p. 169 - 195.
- [12] KLIMESCH, W., SAUSENG, P., HANSLMAYR, S. EEG alpha oscillations: the inhibition-timing hypothesis. *Brain Research Reviews*, 2007, vol. 53, no. 1, p. 63 - 88.
- [13] LU, C.-F., TENG, S., HUNG, C.-I., TSENG, P.-J., LIN, L.-T., LEE, P.-L., WU, Y.-T. Reorganization of functional connectivity during the motor task using EEG time-frequency cross mutual information analysis. *Clinical Neurophysiology: Official Journal of the International Federation of Clinical Neurophysiology*, 2011, vol. 122, no. 8, p. 1569 - 1579.
- [14] LUXBURG, U. A tutorial on spectral clustering. *Statistics and Computing*, 2007, vol. 17, no. 4, p. 395 - 416.
- [15] MODDEMEIJER, R. On estimation of entropy and mutual information of continuous distributions. *Signal Processing*, 1989, vol. 16, no. 3, p. 233 - 248.
- [16] MORMANN, F., LEHNERTZ, K., DAVID, P., ELGER, C. E. Mean phase coherence as a measure for phase synchronization and its application to the EEG of epilepsy patients. *Physica D: Nonlinear Phenomena*, 2000, vol. 144, no. 3-4, p. 358 - 369.
- [17] PALVA, S., PALVA, J. M. New vistas for alpha-frequency band oscillations. *Trends in Neurosciences*, 2007, vol. 30, no. 4, p. 150 - 158.
- [18] ROSSO, O., MARTIN, M., PLASTINO, A. Brain electrical activity analysis using wavelet-based informational tools. *Physica A: Statistical Mechanics and its Applications*, 2002, vol. 313, no. 3-4, p. 587 - 608.
- [19] SAUSENG, P., KLIMESCH, W., DOPPELMAYR, M., PECHERSTORFER, T., FREUNBERGER, R., HANSLMAYR, S. EEG alpha synchronization and functional coupling during top-down processing in a working memory task. *Human Brain Mapping*, 2005, vol. 26, no. 2, p. 148 - 155.
- [20] SCHEERINGA, R., PETERSSON, K. M., OOSTENVELD, R., NORRIS, D. G., HAGOORT, P., BASTIAANSEN, M. C. M. Trial-by-trial coupling between EEG and BOLD identifies networks related to alpha and theta EEG power increases during working memory maintenance. *NeuroImage*, 2009, vol. 44, no. 3, p. 1224 - 1238.
- [21] SCHLOGL, A., KEINRATH, C., SCHERER, R., FURTSCHHELLER, P. Information transfer of an EEG-based brain computer interface. In *First International IEEE EMBS Conference on Neural Engineering*. Capri Island (Italy), 2003, p. 641 - 644.
- [22] SHEN, X., PAPADEMETRIS, X., CONSTABLE, R. T. Graph-theory based parcellation of functional subunits in the brain from resting-state fMRI data. *NeuroImage*, 2010, vol. 50, no. 3, p. 1027 - 1035.
- [23] SHI, J., MALIK, J. Normalized cuts and image segmentation. *IEEE Transactions on Pattern Analysis and Machine Intelligence*, 2000, vol. 22, no. 8, p. 888 - 905.
- [24] SPORNS, O., HONEY, C. J. Small worlds inside big brains. *Proceedings of the National Academy of Sciences of the United States of America*, 2006, vol. 103, no. 51, p. 19219 - 19220.
- [25] TALLON-BAUDRY, C., BERTRAND, O., FISCHER, C. Oscillatory synchrony between human extrastriate areas during visual short-term memory maintenance. *The Journal of Neuroscience: The Official Journal of the Society for Neuroscience*, 2001, vol. 21, no. 20.
- [26] TULADHAR, A. M., TER HUURNE, N., SCHOFFELEN, J.-M., MARIS, E., OOSTENVELD, R., JENSEN, O. Parieto-occipital sources account for the increase in alpha activity with working memory load. *Human Brain Mapping*, 2007, vol. 28, no. 8, p. 785 - 792.
- [27] VAN DEN HEUVEL, M., MANDL, R., HULSHOFF POL, H. Normalized cut group clustering of resting-state fMRI data. *Plos One*, 2008, vol. 3, no. 4.

## About Authors...

**Cagatay AYDIN** was born in Eskisehir, Turkey. He received his B.Sc. from Electronics Engineering Department, Işık University, Istanbul, Turkey in 2010. He received his M.Sc. from Institute of Biomedical Engineering, Bogaziçi University, Istanbul, Turkey in 2012. Now, He is a Ph.D. student in Doctoral School of Biomedical Sciences, Katholieke Universiteit Leuven, Belgium. His research interests include EEG, electrophysiology, graph theory, information theory and vision science.

**Oytun OKTAY** was born in Ankara, Turkey and obtained his bachelors degree in electronics engineering from Gebze Institute of Technology, Kocaeli, Turkey in 2008 with a insight of numerical electromagnetics. Now he is working as a research assistant on the subject of functional brain networks in Electronics and Communication Engineering Department, Namık Kemal University, Çorlu, Turkey.

**Adem Umüt GUNEBAKAN** was born in Istanbul, Turkey. He received his B.Sc. from Electronics Engineering Department, Işık University, Istanbul, Turkey in 2009. He received his M.Sc. from Institute of Biomedical Engineering, Bogaziçi University, Istanbul, Turkey in 2011. Now, He is a Ph.D. student at the same institution. His research interests include EEG, Graph Theory, Neuromarketing.

**Ahmet ADEMOGLU** was born in Diyarbakir, Turkey. He received the B.Sc. degree from the Department of Electrical-Electronics Engineering, and M.Sc. and PhD degrees from the Institute of Biomedical Engineering, Bogaziçi University, Turkey. He is currently the rector of Istanbul Şehir University, Turkey. His research interests are Neuroimaging, Computational Neuroscience and Neuroinformatics.

**Koray CIFTCI** received the B.Sc. degree from the Department of Electrical-Electronics Engineering, and M.Sc. and PhD degrees from the Institute of Biomedical Engineering, Bogaziçi University, Turkey. He is currently an associate professor in the Department of Biomedical Engineering, Namık Kemal University, Turkey. His research interests are biomedical signal processing, cognitive systems and medical instrumentation.